JOURNAL OF SOLID STATE CHEMISTRY 85, 15–22 (1990)

Irradiation-Induced Phase Transition in $Ba_2Fe_2O_5$

J. M. GONZÁLEZ-CALBET,* M. PARRAS, AND M. VALLET-REGÍ

Departamento de Química Inorgánica, Facultad de Ciencias Químicas, Universidad Complutense, 28040 Madrid, Spain

AND J. C. GRENIER

Laboratoire de Chimie du Solide du C.N.R.S., 33405 Talence-Cedex, France

Received February 27, 1989; in revised form October 30, 1989

Monoclinic $Ba_2Fe_2O_5$ is beam-sensitive and readily suffers a nonreversible phase transition during TEM observations. The new phase seems to be an orthorhombic perovskite superlattice with unit cell parameters $a_c\sqrt{3}$, $a_c\sqrt{2}$, $a_c\sqrt{6}$, a_c being the cubic perovskite subcell parameter.

Introduction

A variety of chemical and structural processes can take place in a sample, when it is subjected to the conditions of electron bombardment and high vacuum during observation in a modern high resolution electron microscope (*1*). The addition of low light TV cameras and video recording equipment has led to the observation of dynamic restructuring phenomena resulting principally from electron irradiation of the specimen in the microscope. Since the early study by Hashimoto *et al.* (*2*) on the defect motion in gold foils, several studies of dynamic events on the atomic scale in crystalline materials have been performed such as defect annealing in cadmium telluride (*3*) or structural degradations in the β''' phase of potassium ferrite (*4*), but most efforts have been devoted to study different surface phenomena either on oxides or small particles (*5–13*).

Observations of many oxides under high beam current conditions also cause some interesting beam-induced phase transitions. These transformations can be accompanied by a composition change, as in $Ca_2La(Fe^{3+},Fe^{4+})_3O_{8+z}$ perovskite-related oxide, where the reduction process observed under the electron beam ($Fe^{4+} + e^- \rightarrow Fe^{3+}$) leads to the decomposition in $Ca_2Fe_2O_5$ and $LaFeO_3$ (*14*). However, other perovskite-related oxides show reversible phase transitions without composition change as in $Sr_2Co_2O_5$ brownmillerite-type where a displacement of the oxygen atoms under the electron beam seems to occur leading to the formation of a new phase showing the same composition (*15*).

From our study on the $BaFeO_{3-y}$ perovskite-related system, we have determined, by means of X-ray and electron diffraction, that $Ba_2Fe_2O_5$ shows a multiple

* To whom correspondence should be addressed.

0022-4596/90 $3.00

perovskite superlattice (*16*) which can be indexed on the basis of a monoclinic cell with parameters a = 6.969(1) Å; b = 11.724(1) Å; c = 23.431(1) Å; and β = 98.74(1)°. This phase seems to be very sensitive to the electron beam and suffers from structural changes during TEM observations. We describe in this paper the irradiation effects on monoclinic $Ba_2Fe_2O_5$.

Experimental

$Ba_2Fe_2O_5$ was prepared as described in Ref. (*17*).

TEM observations were performed on a JEOL 200 CX electron microscope, kindly lent to us by the INPG (Grenoble, France), equipped with a side-entry double tilting specimen holder. Specimens were prepared by grinding under *n*-butanol; a drop of suspension was then transferred to a holey carbon support film. Individual crystals were aligned so that the electron beam was parallel to one of the main orientations of crystallographic interest, namely $[100]_m$ and $[010]_m$ (subindex m refers to the monoclinic cell).

Results

As we have previously described (*18*), $Ba_2Fe_2O_5$, being a perovskite-type superstructure, crystallizes on a monoclinic cell. Figure 1a shows the electron diffraction pattern corresponding to the $[100]_m//[1\bar{1}\bar{1}]_c$ zone axis (subindex c refers to the basic perovskite cubic subcell). Two superlattices of the perovskite substructure are seen: a 14-fold superlattice along $[211]_c^*$ and a 4-fold superlattice along the $[01\bar{1}]_c^*$ perovskite direction. When the sample is left for a few minutes within the microscope under normal observation conditions a structural transformation takes place, as observed in both electron diffraction patterns and structure images. This transformation can be accelerated by increasing the beam intensity, but the initial situation is not recovered when such intensity is decreased. It is, then, a nonreversible transition.

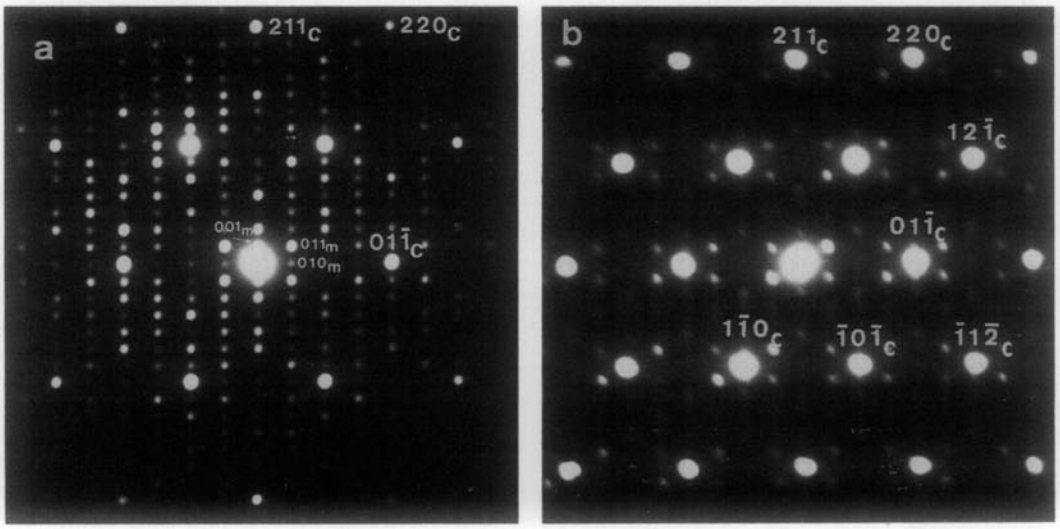

FIG. 1. (a) Electron diffraction pattern of monoclinic $Ba_2Fe_2O_5$ along the $[100]_m//[1\bar{1}\bar{1}]_c$ zone axis. (b) Electron diffraction pattern along the same direction after transformation under the electron beam.

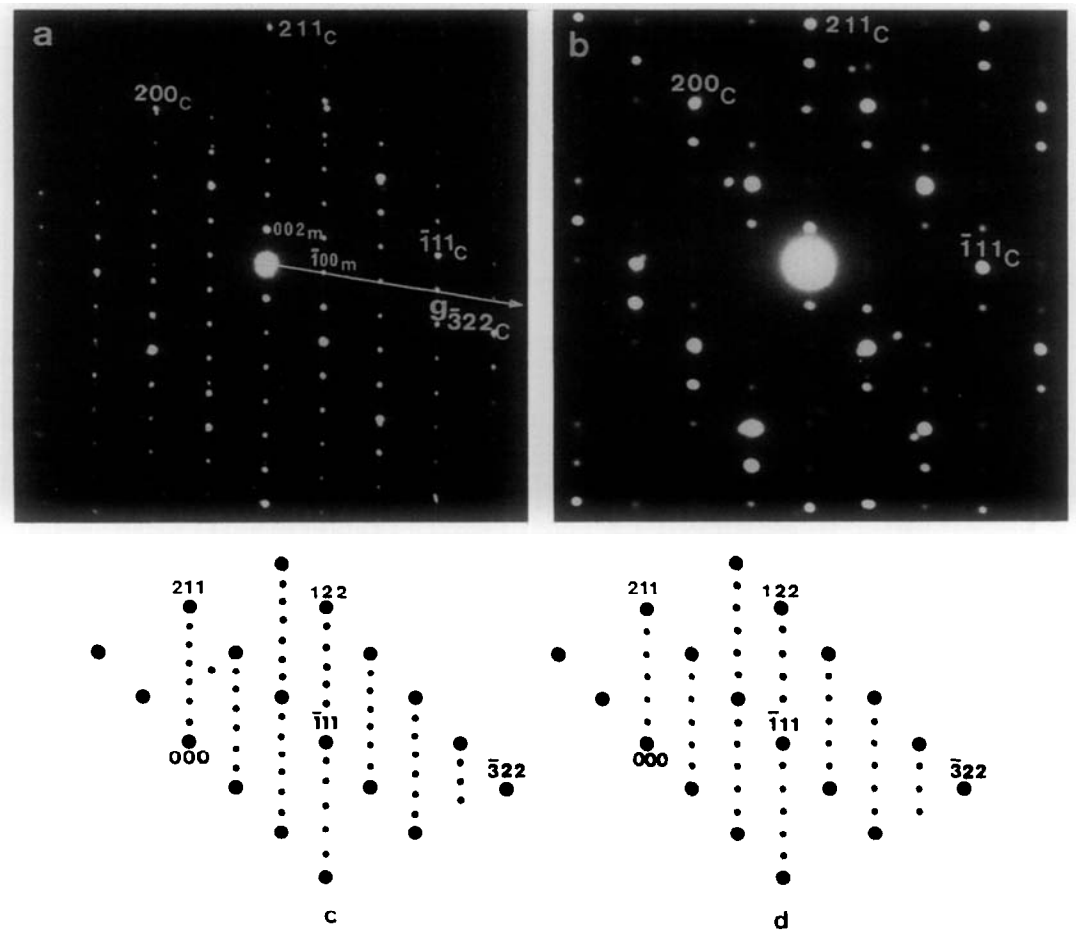

FIG. 2. (a) Electron diffraction pattern along the $[010]_m$ zone axis, equivalent to the $[0\bar{1}\bar{1}]_c$ direction. (b) Diffraction pattern along $[01\bar{1}]_c$ after transformation. (c) Schematic representation of the pattern shown in a. (d) Schematic representation of the pattern shown in b.

Figure 1b shows the electron diffraction pattern along the same $[11\bar{1}]_c$ zone axis after the transformation. Now, the two perovskite-type superlattices are different: a sixfold superlattice along $[211]_c^*$ and equivalent directions, and a twofold superstructure along the $[01\bar{1}]_c^*$ and equivalent directions are seen.

Figures 2a and 2b show the electron diffraction pattern along the $[01\bar{1}]_c$ zone axis before and after the transformation, respectively. As schematically represented in Figs. 2c and d, it can be seen that the sevenfold superlattice along $[3\bar{2}\bar{2}]_c^*$ observed in monoclinic $Ba_2Fe_2O_5$ disappears in the transformed phase. On the other hand, a new threefold superlattice along $[1\bar{1}\bar{1}]_c^*$ appears.

Figure 3 shows a sequence of images along $[1\bar{1}\bar{1}]_c$, illustrating the progressive transformation under the electron beam. Positions and spacing of the fringes do not alter with further irradiation. At the final transformation stage (Fig. 3d), the presence of domains tilted between them 60° can be detected. According to that, the corre-

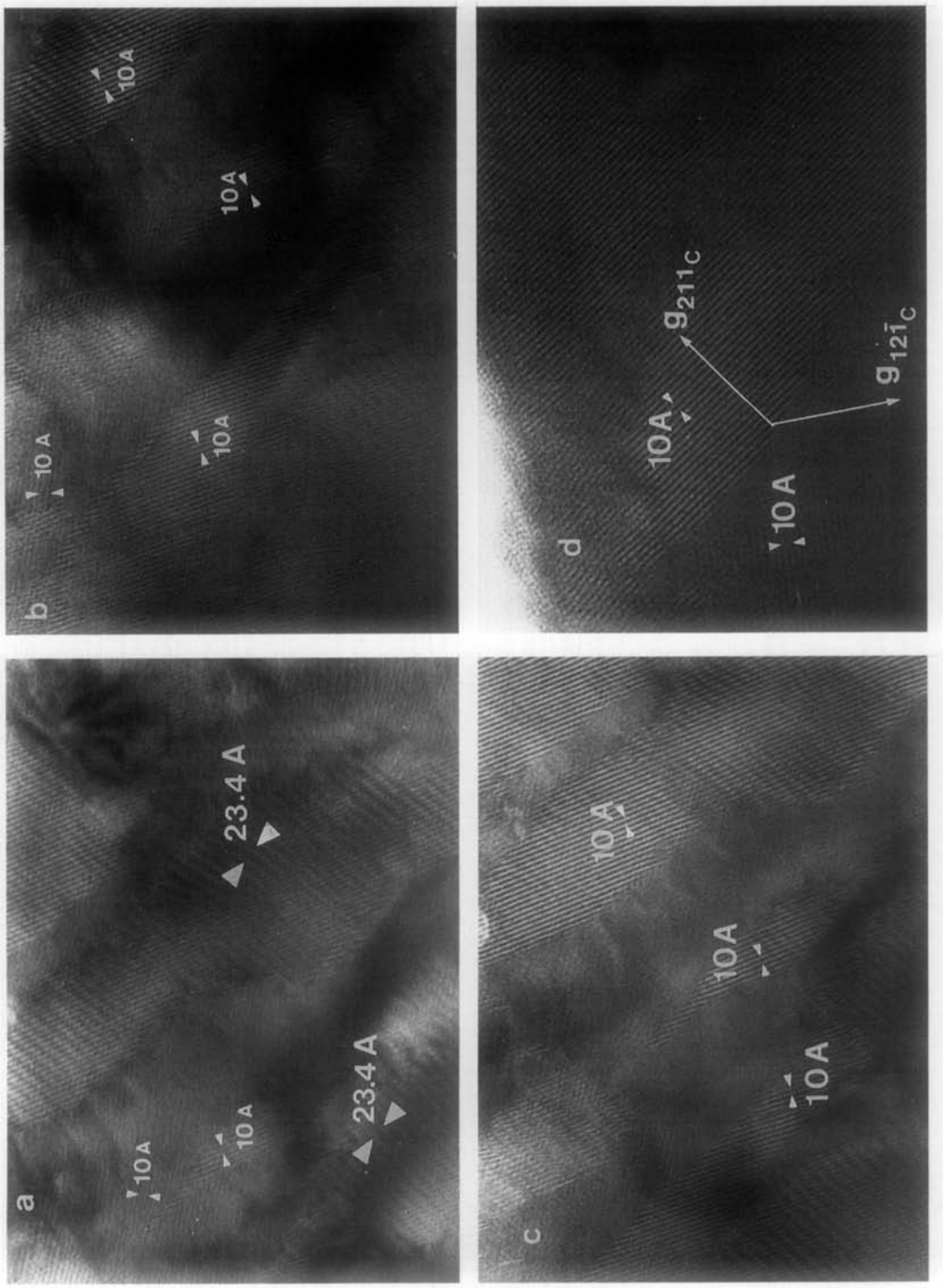

FIG. 3. Four images of $Ba_2Fe_2O_5$ along $[1\bar{1}\,\bar{1}]_c$ taken at intervals of about 1 min showing the progressive transformation of an original crystal initially showing monoclinic symmetry.

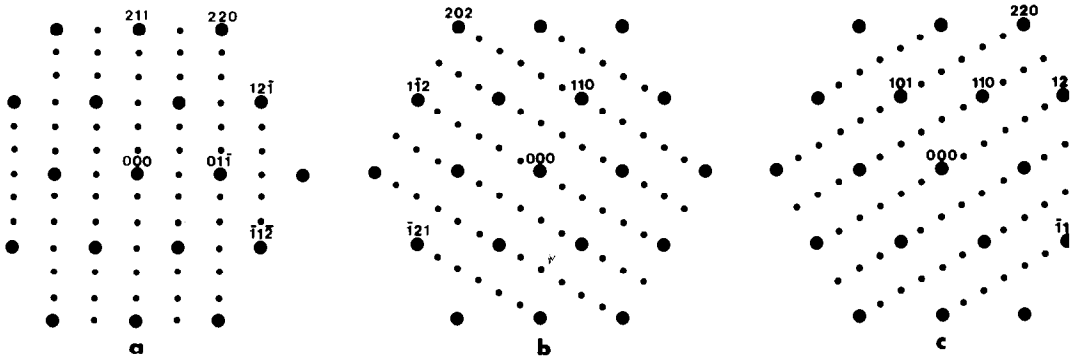

FIG. 4. Schematic representation of the three electron diffraction patterns shown in Fig. 1b showing a sixfold superlattice along $[211]_c$ and equivalent directions.

sponding electron diffraction pattern (Fig. 1b) can be interpreted on the basis of the juxtaposition of three patterns in which the long axis ($6xg_{211c}$) is located along the three [211] cubic directions which form 60° between them, as schematized in Fig. 4. The reciprocal cells corresponding to each domain are represented in Figs. 5a, 5b, and 5c, and are related to the cubic subcell according to the following expressions:

$$\begin{array}{lll} a_o^* = 1/3[1\bar{1}\bar{1}]_c^* & a_o^* = 1/3[1\bar{1}1]_c^* & a_o^* = 1/3[\bar{1}\bar{1}1]_c^* \\ b_o^* = 1/2[01\bar{1}]_c^* & b_o^* = 1/2[110]_c^* & b_o^* = 1/2[101]_c^* \quad (1) \\ c_o^* = 1/6[211]_c^* & c_o^* = 1/6[1\bar{1}2]_c^* & c_o^* = 1/6[12\bar{1}]_c^* \\ \text{Domain A} & \text{Domain B} & \text{Domain C} \end{array}$$

The angles formed between the three reciprocal parameters are 90° and a ≠ b ≠ c indicating that, in each domain, the symmetry of the cell is orthorhombic. The reciprocal cell corresponding to the new phase, as represented in Fig. 6, will be a consequence of the juxtaposition of the three reciprocal domains A, B, and C, giving a hexagonal pseudosymmetry.

From these results, a relationship between the direct cells can be obtained. Thus, for Domain A,

$$\begin{bmatrix} a \\ b \\ c \end{bmatrix}_o = \begin{bmatrix} 1 & \bar{1} & \bar{1} \\ 0 & 1 & \bar{1} \\ 2 & 1 & 1 \end{bmatrix} \begin{bmatrix} a \\ b \\ c \end{bmatrix}_c, \quad (2)$$

where subindex o refers to the orthorhombic cell. From expression (2), the following relationship between the orthorhombic and pseudocubic unit cell parameters can be obtained:

$$\bar{a}_o = \bar{a}_c - \bar{b}_c - \bar{c}_c = \sqrt{3}a_c \approx 7 \text{ Å};$$
$$\bar{b}_o = \bar{b}_c - \bar{c}_c = \sqrt{2}a_c \approx 5.7 \text{ Å};$$
$$\bar{c}_o = 2\bar{a}_c + \bar{b}_c + \bar{c}_c \approx 10 \text{ Å}.$$

Discussion

Structural changes under the electron beam can be accompanied by a reduction process (*14, 19, 20*), since oxidized samples can be reduced within the microscope under normal observation conditions by the combined influence of both high vacuum ($\approx 10^{-6}$ Torr) and the electron beam.

The reduction of the $Ba_2Fe_2O_5$ phase is only possible, according to Neu (*21, 22*), by working at high temperature (≈1000°C) and very low oxygen pressure. In these conditions, $Ba_2Fe_2O_5$ can only be reduced to $BaFeO_{2.49}$, no changes in the symmetry being observed. When a higher degree of reduction is attained, the material decomposes leading to the formation of metallic iron. However, the condition of a sample under the electron beam irradiation in TEM significantly differs from those of conventional experiments of solid state reactions

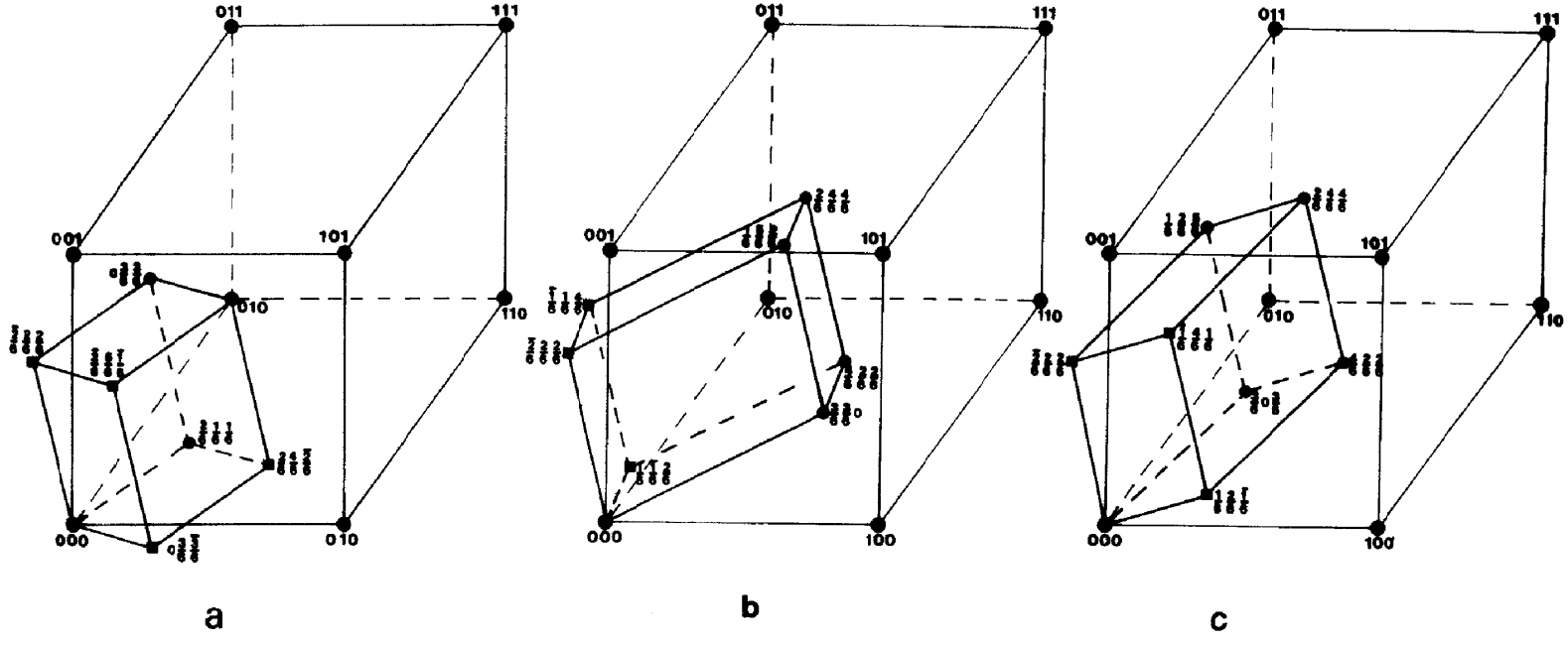

FIG. 5. Schematic reciprocal unit cells of *A* (a), *B* (b), and *C* (c) domains.

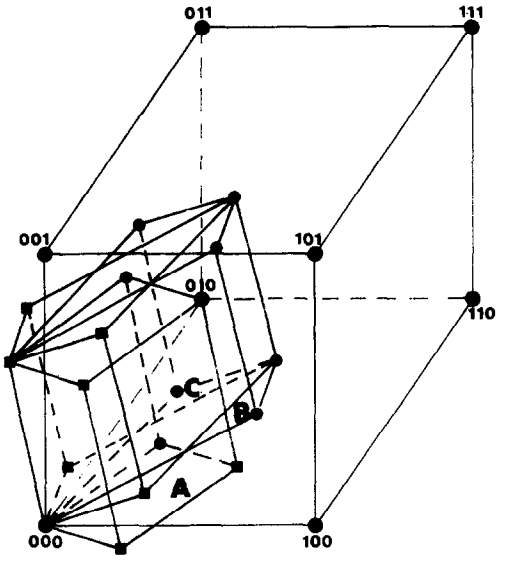

FIG. 6. Schematic reciprocal unit cell of the orthorhombic phase showing the juxtaposition of *A*, *B*, and *C* domains related to the cubic perovskite subcell.

due to the use of an extremely thin sample and irradiation of high energy charged particles (*23*). Hence both experiments cannot simply be compared with each other.

Although the experimental conditions under the electron beam seem to favor a reduction process, some oxidation reactions have been described in such circumstances. This is so in the case of partial oxidation on the surface of several oxides (*24*). However, it seems difficult to justify, under these conditions, the whole structural transformation observed in $Ba_2Fe_2O_5$ as a consequence of an oxidation process.

The chemical composition of the new phase has been analyzed in a JEOL 2000 FX electron microscope fitted with an ultrathin window-energy dispersive X-ray spectrometer (Link analytical AN 1000 10/55 S). No compositional change is observed with respect to the monoclinic phase. However, if there is a very slight change of chemical composition, such a difference could be included in the error range of the measurement (*25*). Further analysis is necessary to clarify this point.

On the other hand, either the local temperature on the crystal or the impulse transference of the electrons can produce a rearrangement of the atoms leading to a different state of order. Although the monoclinic $Ba_2Fe_2O_5$ structure is not yet known and we do not have diffusion data for this material, there exist some diffusion results of perovskite-type compounds indicating that *M* cations are the slowest among the three ions constituting AMO_3 solids (*26, 27*). In fact, in the whole transformation process the *M* sublattice, which in the perovskite constitutes a simple cubic lattice, remains fixed since the strong reflections characteristic of the perovskite substructure do not change. Regarding the barium atomic number it seems reasonable that oxygen atoms will move somewhat faster in $Ba_2Fe_2O_5$ so a rearrangement of the lightest atoms can produce a new anionic sublattice.

From these results the nonreversible transformation of the monoclinic $Ba_2Fe_2O_5$ leads to a new phase showing orthorhombic symmetry. It is worth mentioning that Ichida (*28*) has studied the decomposition of $BaFeO_4$ in air, obtaining two different phases where all iron is in state oxidation III. The first one has been indexed as triclinic by Mori (*29*) although our recent study by electron diffraction (*18*) shows this phase to be monoclinic. We cannot compare the second one, called "low-temperature $BaFeO_{2.50}$," since its unit cell has not been determined.

We have tried to prepare the orthorhombic phase by several methods under different experimental conditions, but with unsuccessful results up to now. It seems, then, that only on the conditions experienced under the electron beam is it possible to stabilize such a phase.

References

1. L. W. HOBBS, "Quantitative Electron Microscopy" (J. N. Chapman and A. I. Craven, Eds.), p. 399 (SUSSP, Edinburgh. (1984).
2. H. HASHIMOTO, Y. YOKOTA, Y. TAKAI, M. ENDOH, AND A. KUMAO, *Chem. Scr.* **14,** 125 (1978/1979).
3. R. SINCLAIR, E. A. PONCE, T. YAMASHITA, D. J. SMITH, R. A. CAMPS, L. A. FREEMAN, S. F. ERASMUS, K. C. A. SMITH, W. C. NIXON, AND C. I. D. CATTO, *Nature (London)* **298,** 127 (1982).
4. Y. MATSUI, Y. BANDO, Y. KITAMI, AND R. S. ROTH, *Acta Crystallogr. B* **41,** 27 (1985).
5. L. A. BURSILL, P. J. LIN, D. J. SMITH, AND I. E. GREY, *Inst. Phys. Conf. Ser.* **78,** 463 (1985).
6. D. J. SMITH, *Inst. Phys. Conf. Ser.* **78,** 311 (1985).
7. J. O. BOVIN, L. R. WALLENBERG, AND D. J. SMITH, *Inst. Phys. Conf. Ser.* **78,** 481 (1985).
8. J. O. BOVIN, *Proc. XIth Int. Conf. Electron Microsc. Kyoto* **1,** 83 (1986).
9. S. IJIMA, *Proc. XIth Int. Conf. Electron Microsc. Kyoto* **1,** 87 (1986).
10. L. D. MARKS, *Proc. XIth Int. Conf. Electron Microsc. Kyoto* **1,** 91 (1986).
11. D. J. SMITH, *Proc. XIth Int. Conf. Electron Microsc. Kyoto* **2,** 929 (1986).
12. D. WHITE, J. L. HUTCHISON, AND S. RAMDAS, *Int. Phys. Conf. Ser.* **90,** 249 (1987).
13. S. HANSEN AND D. J. SMITH, *Int. Phys. Conf. Ser.* **90,** 151 (1987).
14. J. M. GONZÁLEZ-CALBET, M. VALLET-REGI, AND M. A. ALARIO-FRANCO, *J. Solid State Chem.* **60,** 320 (1985).
15. J. M. GONZÁLEZ-CALBET AND J. RODRIGUEZ, *Inst. Phys. Conf. Ser.* **93,** 379 (1988).
16. M. PARRAS, Doctoral thesis, Complutense University of Madrid, Spain (1988).
17. J. C. GRENIER, A. WATTIAUX, M. POUCHARD, P. HAGENMULLER, M. PARRAS, M. VALLET, J. CALBET, AND M. ALARIO-FRANCO, *J. Solid State Chem.* **80,** 6 (1989).
18. M. PARRAS, M. VALLET-REGI, J. M. GONZÁLEZ-CALBET, M. A. ALARIO-FRANCO, J. C. GRENIER, AND P. HAGENMULLER, *Mater. Res. Bull.* **22,** 1413 (1987).
19. C. BOULESTEIX AND L. EYRING, *J. Solid State Chem.* **66,** 125 (1987).
20. C. BOULESTEIX AND L. EYRING, *J. Solid State Chem.* **75,** 291 (1988).
21. P. NEU, Doctoral thesis, Nancy University (1969).
22. P. NEU, M. ZANNE, AND C. GLEITZER, *J. Solid State Chem.* **36,** 205 (1981).
23. "High Resolution Transmission Electron Microscopy and Associated Techniques" (P. Buseck, Ed.), p. 464. Oxford Univ. Press, London/New York.
24. Z. C. KONG, L. EYRING, AND D. J. SMITH, *Proc. XIth Int. Conf. Electron Microsc. Kyoto* **1,** 833 (1986).
25. D. B. WILLIAMS, "Practical Analytical Electron Microscopy in Materials Science," Verlag-Chemie, Weinheim. 1984.
26. I. E. SHIMANOVICH, M. M. PAULYUCHENKO, B. O. FILONOV, AND S. A. PROKUDINA, *Vesti Akad. Navuk B SSR, Ser. Khim. Navuc* No. 6, 61 (1960).
27. I. ISHIGAKI, S. YAMAUCHI, J. MIZUSAKI, K. FUEKI, H. NAITO, AND T. ADACHI, *J. Solid State Chem.* **55,** 50 (1984).
28. T. ICHIDA, *J. Solid State Chem.* **7,** 308 (1973).
29. S. MORI, *J. Amer. Ceram. Soc.* **48,** 165 (1965).